

Osservatorio Astrofisico di Arcetri - Gruppo di Radioastronomia

## An X/K band Dichroic System for Radioastronomical Applications

A. Monorchio<sup>2</sup>, F. Palagi<sup>1</sup>, D. Panella<sup>3</sup>, P. Leto<sup>4</sup>, C. Nocita<sup>4</sup> and N. Fognani<sup>1</sup>

<sup>1</sup> CAISMI - CNR, l.go E. Fermi 5, 50125 Firenze (Italy)

<sup>2</sup> Department of Information Engineering, University of Pisa, I-56126 Pisa (Italy)

<sup>3</sup> Arcetri Astrophysical Observatory, l.go E. Fermi 5, 50125 Firenze (Italy)

<sup>4</sup> IRA - CNR, Noto VLBI Station, I-96017 Noto, Siracusa (Italy)

**Arcetri Technical Report 5/2001**  
**Florence December 2001**

**Abstract** *Within the framework of the RADSPEC project funded by the Italian National Research Council, a dichroic screen for radioastronomical applications has been designed and realized.*

*Its design, although based on the thin type approach, shows the same loss characteristics of those based on the thick type approach, but is much more robust against variations of the radiation incidence angle.*

*The dichroic screen is realized with two thin parallel Frequency Selective Surfaces (FSS). Its transmission band goes from 21 GHz to 26 GHz and the reflection low-frequency cut-off is at 10 GHz. The main advantage of the dual FSS configurations is a wider transmission bandpass as compared to the transmission band of the single FSS.*

*Laboratory tests show a very good agreement with the numerical simulations, confirming the reliability of the design methods and programs.*

*Measurements have been done on each single FSS first and then on the two coupled FSS's set at different distances. The best compromise between the wider transmission bandwidth and the lower average attenuation in the band is obtained with  $d = 4.3$  mm.*

*An astronomical test has been performed at 22.235 GHz with the Noto VLBI Radiotelescope, measuring the antenna temperature of the radio source Taurus A, with and without the dichroic screen. At the same time the system temperature increase due to the dichroic screen was measured.*

*While the atmospheric noise fluctuations prevent a direct measurement of the dichroic screen attenuation, it can be obtained from the system temperature increase due to the screen. The derived value confirms the design and laboratory measurements which are below the design specification of 0.1 dB as a maximum value.*

## Introduction

Multifrequency simultaneous observations of radio emission from astronomical sources are of valuable interest in several applications. For instance, S/X bands observations for geodynamical studies are routinely done by VLBI networks.

Simultaneous single dish observations of the same source at two different frequencies are useful in several respects.

They are required when one needs to correlate phenomena showing a high degree of time variability, such as maser emission from molecules associated with star forming regions or late-type stars.

They reduce significantly the observation time, that may become too long when measurements at two different frequencies are required either on a large sample of sources or for long integration times.

Simultaneous observations of the same source at two frequencies can be accomplished via the use of a dichroic screen put on top of the feed accepting the transmitted radiation. A suitable mirror system is used to convey the reflected radiation to the second feed.

Due to the extremely low power levels of the radioastronomical signals, the contribution of the dichroic screen to the system noise temperature has to be minimized. Dichroic surfaces installed on radiotelescopes are typically screens of thick metallic type to reduce their ohmic losses. However they are heavy, their fabrication is difficult and the radiation incidence angle is almost fixed.

Using a thin type approach, a new frequency selective surface (FSS) has been designed and realized, which satisfies the requirements of a low contribution to the system noise temperature, has a high tolerance to the incidence angle of the radiation and has a wide transmission bandwidth.

This dichroic screen was developed and realized within the RADSPEC project, funded by the italian National Research Council (CNR).

## 1 Design description

In this section we review the main characteristics of the FSS design with particular attention to the expected frequency response. A more detailed description is given in [1].

The screen is designed to operate in front of the K-band receivers of the Medicina and Noto radiotelescopes in the Cassegrain mounting configuration. The total beam aperture of the feeds is  $18^\circ$  and the expected incidence angle of the radiation is  $25^\circ$ .

The astronomical frequencies of main interest are 22.3 GHz ( $\text{H}_2\text{O}$  maser line) in the K band, and 8.6 GHz ( $^3\text{He}$  recombination line) and 6.7 GHz ( $\text{CH}_3\text{OH}$  maser line) in the X band. The bandwidth in K should be wide enough to allow the observations of the 23.6 GHz  $\text{NH}_3$  line.

Preliminary investigations showed that a single screen could not meet the wide bandpass specification of the project, so that a dual screen solution

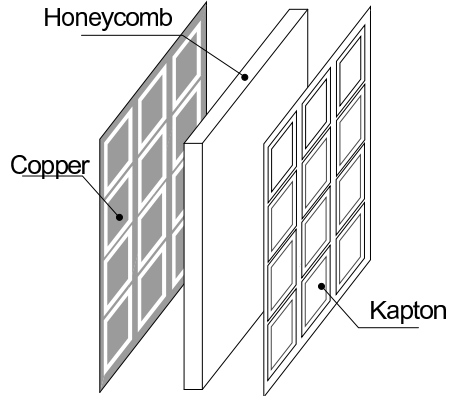


Figure 1: Design layout of the dual screen solution.

has been considered.

The first version of the dual screen design is sketched in fig. 1, taken from [1]. The screen is a combination of two thin FSS's each one composed of an array of square loop cells (fig. 2), kept at a distance of 4.0 mm by a Kevlar honeycomb layer. The cell dimensions are  $d_x = 3.3 \text{ mm}$  and  $d_y = 4.67 \text{ mm}$ .

The computed power and phase response of the screen versus frequency, is reported in fig. 3.

## 2 Realization

Each FSS is 35 cm wide by 40 cm high, as required by the feed geometry.

MBF<sup>1</sup>, the factory selected for the realization of the screen, has proposed a mounting system that makes the Kevlar honeycomb no longer necessary. Each FSS is stretched and glued on a polyester textile which, in turn, is glued on an aluminium frame. The frame dimensions are 50 cm by 50 cm. The two frames are kept at the required distance by three shims of the suitable thickness, and are covered by ecosorb panels, to avoid reflections.

The cell dimensions are modified to  $d_x = 3.8 \text{ mm}$  and  $d_y = 4.2 \text{ mm}$ , to take into account the removal of the Kevlar honeycomb.

Each FFS is realized by photoengraving a 25  $\mu\text{m}$  thick copper layer on a kapton substrate. The cell dimensions were then measured using a graduated microscope, obtaining  $d_x = 3.6 \text{ mm}$  and  $d_y = 4.2 \text{ mm}$ .

---

<sup>1</sup>MBF, v. Ungaretti, 5, I-20063 Cernusco sul Naviglio, Milano, Italy

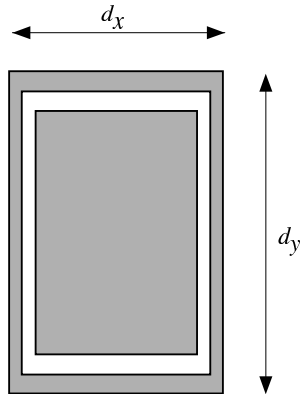


Figure 2: Design layout of the dual screen solution.

### 3 Laboratory tests

Laboratory instrumentation allow us to measure only the transmission pass-band of the screen (K band). Reflection measurements at 8.6 GHz must be done in the near field regime which require an anechoic room larger than the one available at the Arcetri Astrophysical Observatory. However, comparison of the transmission measurements with the simulations can be used to test the degree of accuracy of the design.

In any case, final tests at the the telescope will be performed for both transmission and reflection operations.

#### 3.1 Measurement set-up

The transmission measurement set-up is illustrated in fig. 4. Two square feed horns are set aligned at a distance  $L = 70\text{cm}$  that satisfies the far field condition given by the relation:

$$L > \frac{2 D^2}{\lambda}$$

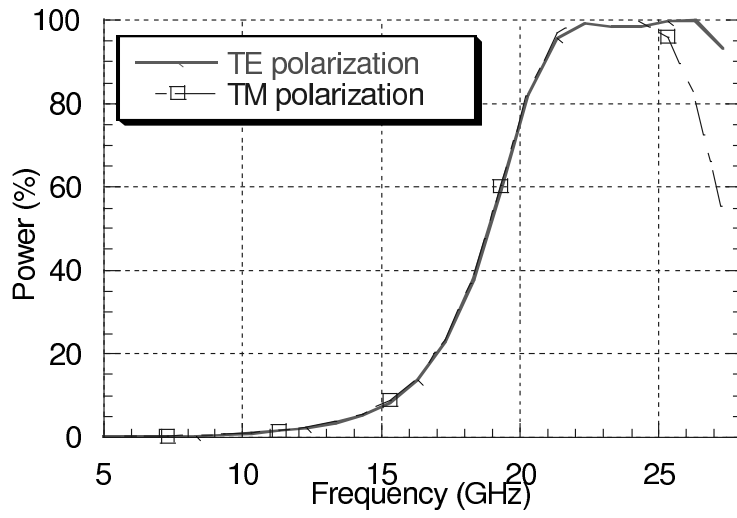
where:

$L$  is the distance between the two horns,

$D$  is the maximum horn aperture,

$\lambda$  is the radiation wavelenght.

In our case  $D = 5 \text{ cm}$ ,  $\lambda = 1.3 \text{ cm}$ , so the minimum horn separation is  $L_m = 38.5 \text{ cm}$ . The horn bearings and any other equipment were also shielded with eccosorb panels.



(a)

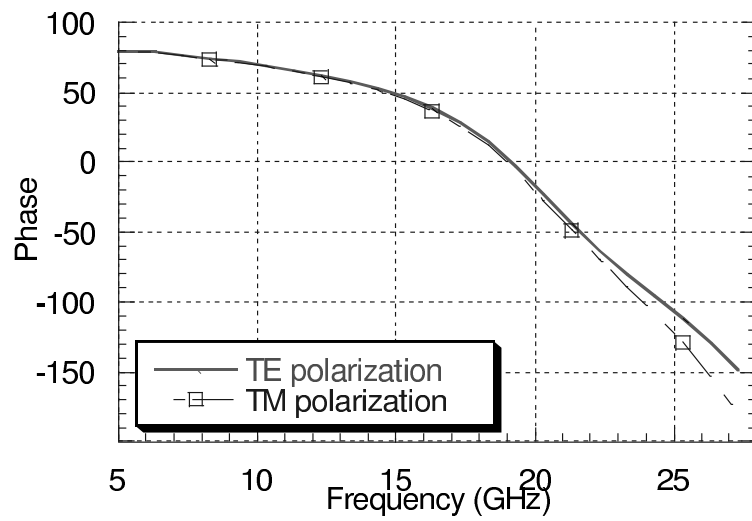


Figure 3: Simulated power and phase transmission spectrum for the dual screen. The distance between the two screens is  $D = 4.0 \text{ mm}$ .

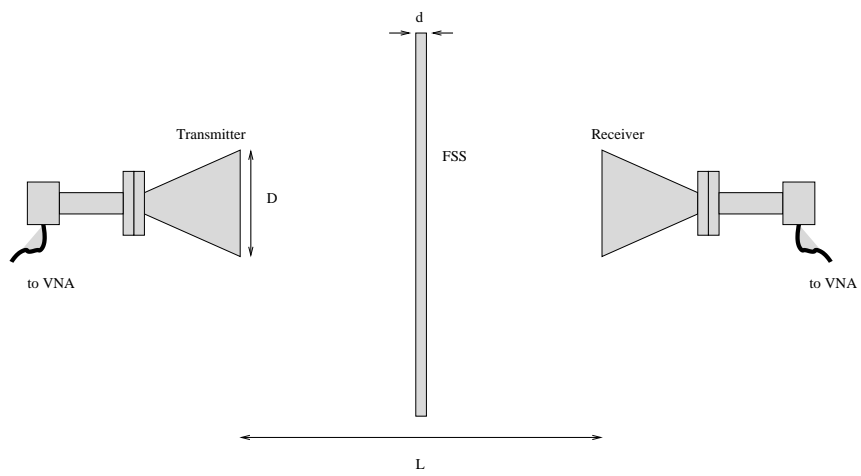


Figure 4: Measurement set-up for the determination of the transmission pass-band of each SSF and of the complete screen. The screen under test is inclined by  $25^\circ$  with respect to the line connecting the two feeds.

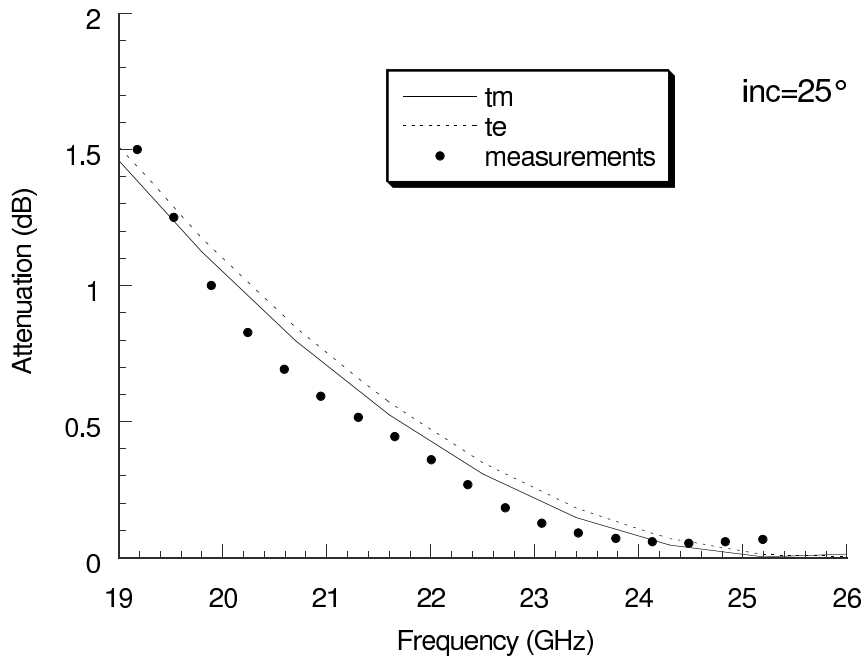


Figure 5: Measurement of the attenuation distribution in TE polarization for a single FSS with an inclination angle of  $25^\circ$ .

A Network Vector Analyser (VNA) Anritzu 37269B covering the band between 19 GHz and 26 GHz has been used to measure the bandpass. All measurements have been done in TE polarization case.

The main design goal is to obtain an attenuation  $\varepsilon < 0.1 \text{ dB}$  over a bandwidth ranging from 22 GHz up to 25 GHz. The FSS attenuation is measured recording the power distribution received by one horn with and without the FSS and computing the ratio between the two's.

The computed attenuation values are then numerically filtered to a frequency resolution comparable to that of the numerical simulations.

As the screen is expected to operate with an inclination angle of  $25^\circ$  its attenuation has been measured with the same inclination with respect to the radiation direction. This set-up has the advantage of substantially removing the standing wave which may arise from any small reflection at the FSS.

### 3.2 Results

First, the attenuation introduced by each single FSS was measured. The



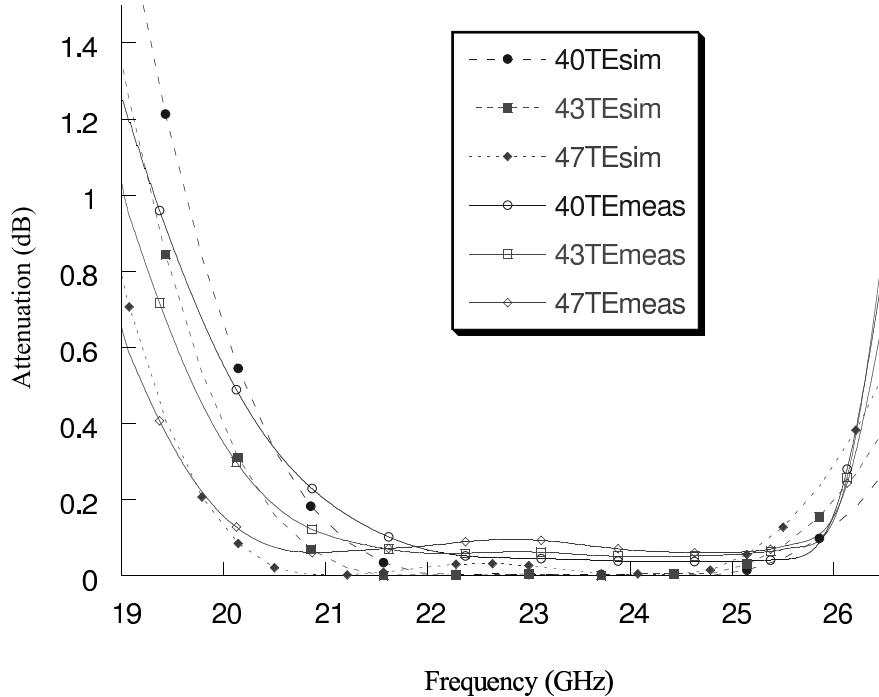


Figure 6: Measurement and simulations of the attenuation distribution in TE polarization for the double FSS screen for 3 different spacings.

resulting attenuation distribution is reported in fig. 5 and compared to the expected distribution.

The difference between the experimental data and the numerical simulations is  $< 0.1db$  all over the required bandpass, which confirm the quality of the design.

Therefore a second set of measurements was obtained with the double FSS screen. As the bandwidth varies with the spacing between the two FSS's, we have used three different shim sets:  $s = 4mm$ ,  $s = 4.3mm$ ,  $s = 4.7mm$ . The corresponding attenuation distributions are plotted in fig. 6. It is apparent that the lower frequency cut-off decreases with increasing spacing values, while the average attenuation value increases.

The same measurements have been done in TM polarization. Figs 7, 8 e 9 reports the attenuation for the two polarizations using the  $s = 4mm$ ,  $s = 4.3mm$  and  $s = 4.7mm$  spacings respectively.

The  $s = 4.0mm$  spacing gives the best depolarization behaviour with the higher low frequency cut-off of 21.5 GHz. A spacing of  $s = 4.3mm$  produces a slightly worse depolarization behaviour over the bandwidth, but

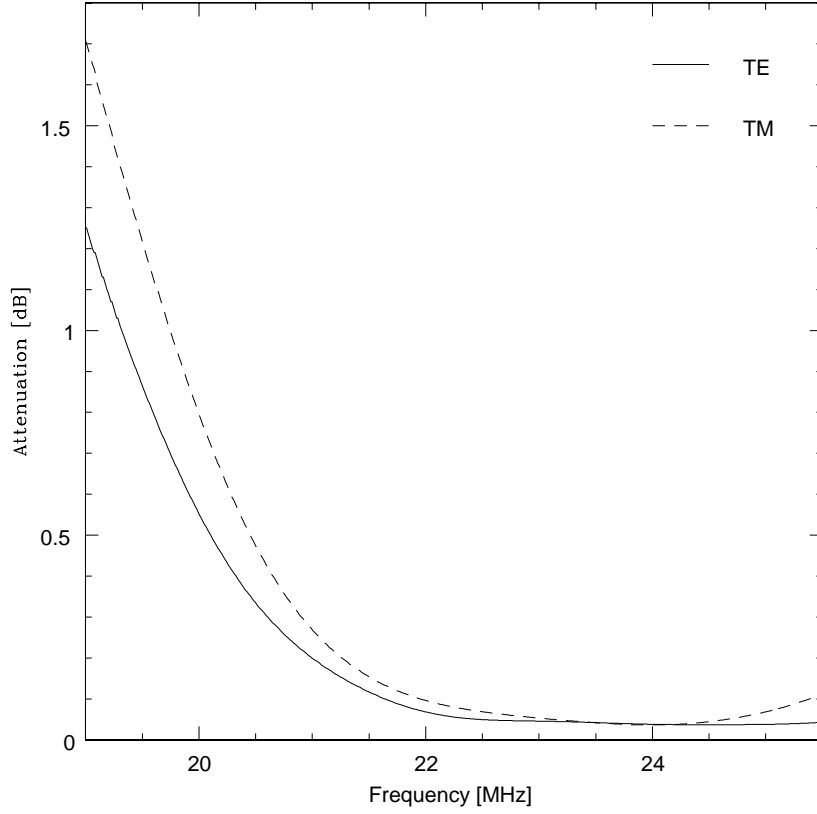


Figure 7: Measurement of the transmitted power distribution in TE and TM polarizations for the double FSS screen with a separation of 4.0 mm.

gives a lower low frequency cut-off, down to 21.0 GHz. The last spacing of  $s = 4.7\text{ mm}$  gives an even wider bandwidth, but with an unacceptable increase of the depolarization over the bandwidth.

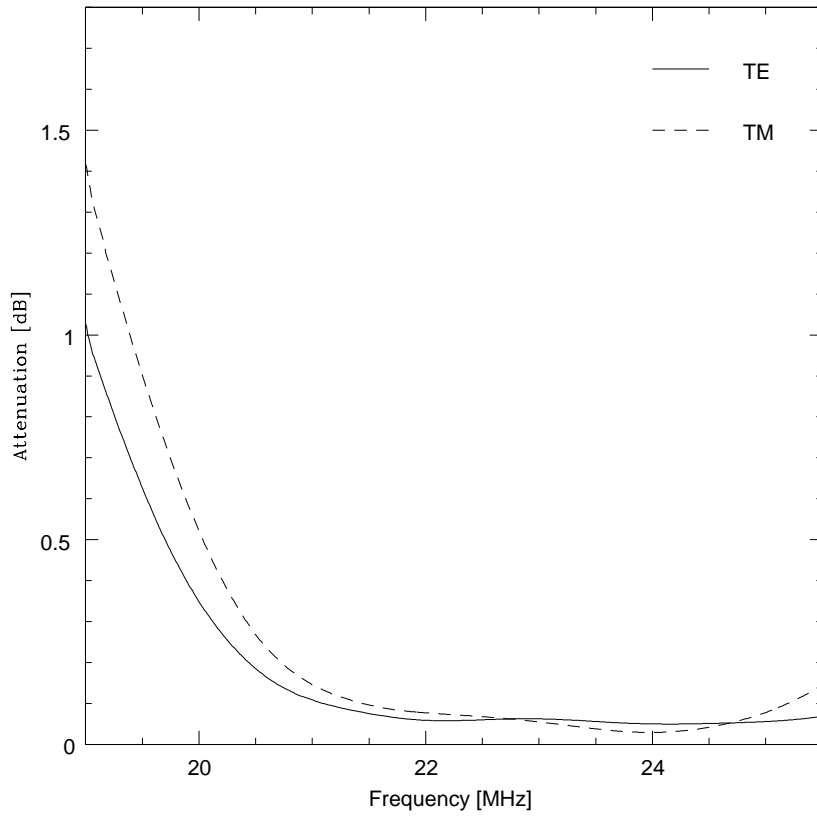


Figure 8: Measurement of the transmitted power distribution in TE and TM polarizations for the double FSS screen with a separation of 4.3 mm.

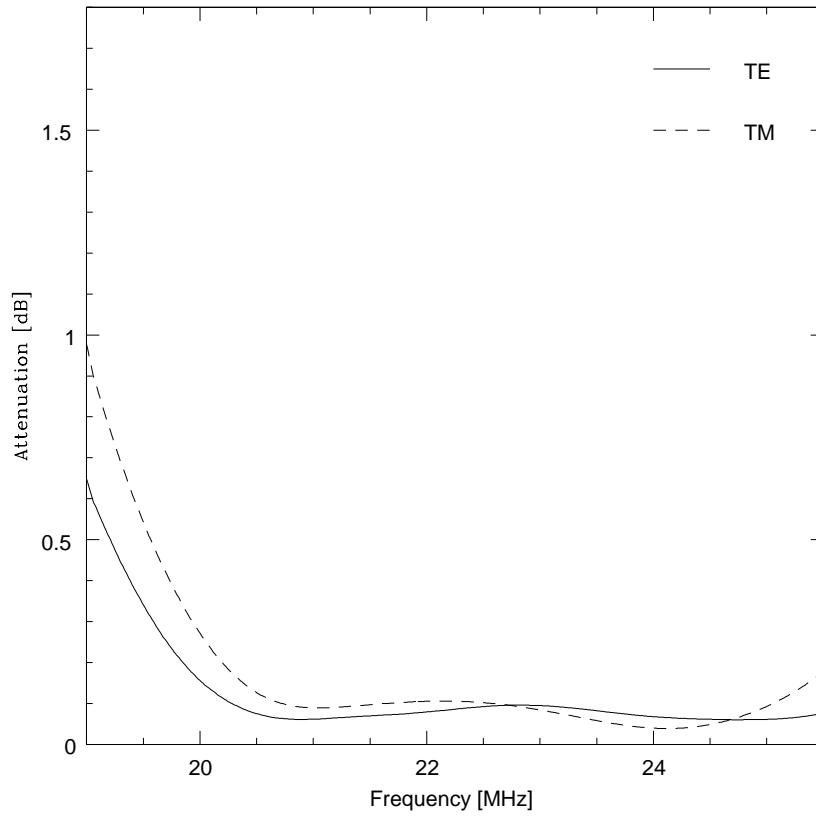


Figure 9: Measurement of the transmitted power distribution in TE and TM polarizations for the double FSS screen with a separation of 4.7 mm.

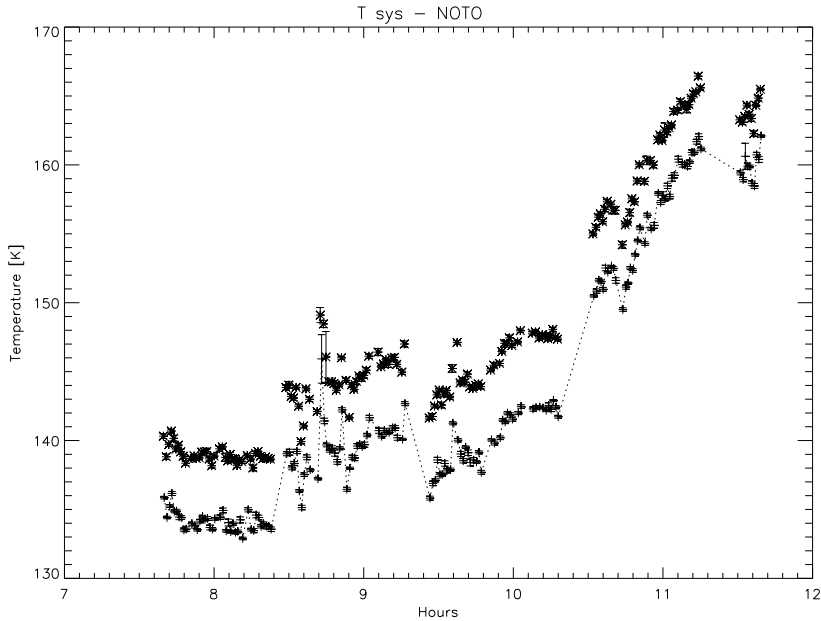


Figure 10: Plot of the system temperature vs. time. The points represent on-source and off-source measurements. The overall temperature increase at Hours=9 UT and Hours = 11 UT is due to the insertion of the dichroic screen.

#### 4 The astronomical test

The Noto VLBI radiotelescope is equipped with a K-band receiver centered on the  $\text{H}_2\text{O}$  line at 22.235 GHz in the Cassegrain focus. This mounting is suitable for an astronomical measurement of the dichroic screen attenuation, although at a single frequency.

The screen was mounted on top of the feed horn using an ad hoc tiltable mechanical structure. To determine the attenuation introduced by the screen, the antenna temperature of source Taurus A was measured with and without the screen, with the position switching mode.

A typical measurement is shown in fig. 10 where a sequence of on-source ( $T_{ON}$ ) and off-source ( $T_{OFF}$ ) measurements of the system temperature  $T_{sys}$  is plotted. The sequence clearly shows the noise temperature increase due to the insertion of the dichroic screen in the two time intervals centered at 9:00 UT and 11:00 UT.

Three sequences like this one have been taken. The antenna temperature  $T_A = T_{ON} - T_{OFF}$ , derived from these measurements does not show any significant variation (fig. 11), as the noise due to the fluctuations of the atmospheric attenuation are much larger than the expected attenuation of

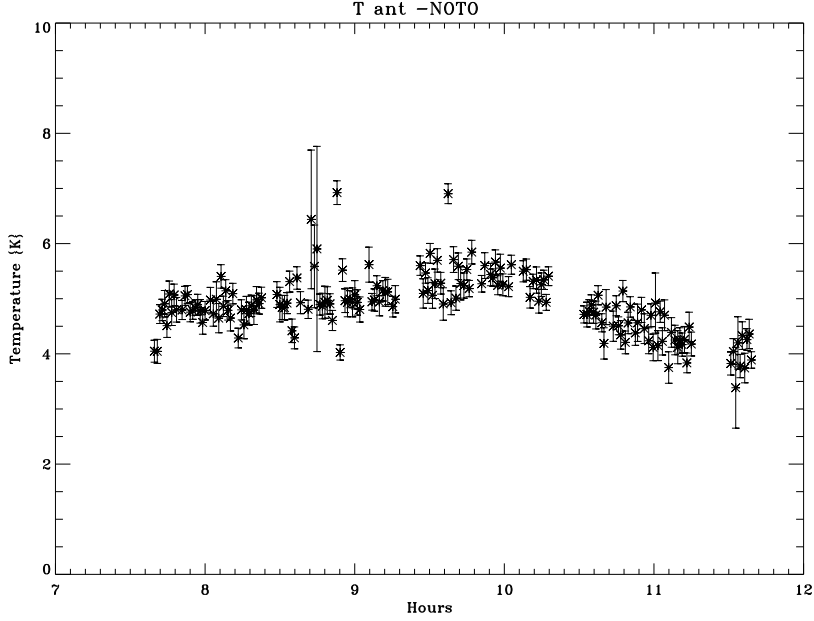


Figure 11: Plot of the antenna temperature vs. time for the source Taurus A. No systematic decrease is observed when the dichroic screen is put on top of the receiver feed.

the dichroic screen.

As already noted, the noise temperature contribution from the screen is measurable and can be used to derive the attenuation due to the screen, based on the simple relation:

$$\Delta T_{sys} = \varepsilon T_{env}$$

where  $\varepsilon$  is the screen attenuation and  $T_{env}$  is the environment temperature assumed to be 300 K. To estimate  $\Delta T$  the  $T_{OFF}$  sequence has been fitted with the following function:

$$T_{sys} = P^n(t_i) + z_i \Delta T$$

where  $P^n(t_i)$  is a third order polynomial and  $z_i = 1$  when the screen is on and  $z_i = 0$  when the screen is off.

The results are summarized in table 1.

The average value is  $\Delta T = 5.3 \pm 0.4K$  which corresponds to an attenuation  $\varepsilon = 0.08dB$ . This value confirms the laboratory measurements and is below the project specifications.

Table 1: Temperature increase due to the dichroic screen.

Sequence	$\Delta T$	Error
1	5.73	0.17
2	5.15	0.37
3	4.93	0.14

## 5 Conclusions

In this report, a realization of a dichroic screen for radioastronomical applications has been illustrated. The overall screen system is made by two FSSs kept at a suitable distance to provide wide band performance. This configuration allowed us to meet the design specifications in terms of attenuation and frequency response. Laboratory transmission measurements are in quite good agreement with the simulated behaviour as far as the attenuation in the K band is concerned. The best compromise between the wider bandwidth and the smaller average attenuation in the band is obtained with a spacing of 4.3 mm between the two FSS. The measured attenuation values are within the required attenuation level of  $\varepsilon < 0.1dB$ .

An astronomical test performed at the frequency  $\nu = 22.235GHz$  with the Noto VLBI Antenna confirms the values measured in the laboratory tests.

Full astronomical tests (wide band transmission in X-band and reflection in K-band) will be performed as soon as a wide band K-band receiver will be available for the Cassegrain mounting in Noto or in Medicina.

## References

- [1] G. Manara, A. Monorchio, A. Talarico, and R. Mittra, 1999, *Design of a Dichroic Surface for Dual-frequency Radioastronomical Observations*, Microwave and Opt. Technol. Lett., 20,126–129